

# Optical detection of magnetic fields using giant magnetoresistance in undoped coupled quantum wells

S. Denev, V. Negoita,\* and D. W. Snoke†

*Department of Physics and Astronomy, University of Pittsburgh, 3941 O'Hara Street,  
Pittsburgh, Pennsylvania 15260*

B. Laikhtman

*Racah Institute of Physics, The Hebrew University, Jerusalem 91904, Israel*

K. Eberl

*Max-Planck-Institut für Festkörperforschung, Heisenbergstrasse 1, 70506 Stuttgart, Germany*

L. Pfeiffer

*Bell Labs, Lucent Technologies 700 Mountain Avenue, Murray Hill, New Jersey*

(Received 9 July 2002; published 6 November 2002)

We show that undoped coupled quantum well structures of GaAs and InGaAs have a magnetoresistance effect which leads to a wavelength shift of the optical spectrum. This effect allows the optical emission to be used to detect magnetic field in the range 0–0.5 T.

DOI: 10.1103/PhysRevB.66.205304

PACS number(s): 72.20.My, 73.21.Fg, 78.67.De, 71.35.Ji

## I. INTRODUCTION

When thinking of a giant magnetoresistance effect, one normally thinks of materials with magnetic properties. In the experiments discussed here, however, we have observed a giant magnetoresistance effect in undoped quantum wells of GaAs and  $\text{In}_x\text{Ga}_{1-x}\text{As}$ . The resistance changes by up to a factor of three as the magnetic field varies from zero to 0.5 T.

The system in which we see this effect is a set of coupled quantum wells with outer barriers, with electric field and magnetic field both applied perpendicular to the wells, as illustrated in Fig. 1. As reported in several other studies,<sup>1–4</sup> the electric field causes a tilting of the bands which leads to spatial separation of electrons and holes into adjacent wells. The excitons formed from these spatially separated electrons and holes are known as “indirect” excitons or “dipole” excitons. An important feature of the luminescence from this type of structure is that the luminescence shifts to lower energy with increasing electric field, in what is known as the “quantum confined Stark effect.” The spectral position of the luminescence from the wells therefore gives a direct measurement of the local electric field.

In 1999, we reported<sup>5</sup> a strong redshift of the luminescence from excitons in GaAs coupled quantum wells in a weak magnetic field. A similar, weaker effect was also reported by Krivolapchuk *et al.*<sup>6</sup> We have also reproduced this effect in  $\text{In}_{0.1}\text{Ga}_{0.9}\text{As}$  coupled quantum wells. Figure 2 shows typical spectra from an  $\text{In}_{0.3}\text{Ga}_{0.7}\text{As}$  coupled quantum well structure, consisting of 60 Å wells with a 40 Å barrier between the wells made of pure GaAs, with  $\text{Al}_{0.3}\text{Ga}_{0.7}\text{As}$  outer barriers, separated from the wells by 50 Å of pure GaAs. The outer barrier on the substrate side is 200 Å thick, and the barrier on the top side is 1000 Å thick. The GaAs substrate and the GaAs capping layer are heavily doped, which allows the electric field to be applied across a relatively thin region of the sample.

As seen in Fig. 2, the shift of the luminescence line with magnetic field is much larger than the linewidth even at relatively weak magnetic fields. We have observed similar behavior in GaAs coupled quantum wells, at the same well width and at different widths, including 80 and 100 Å widths. The energy shift of the luminescence is proportional to  $B^2$  in all cases at low magnetic field. Figure 3 shows the line position of the luminescence from a GaAs coupled quantum well structure as a function of magnetic field, at very low magnetic fields. The solid line is simply a fit to a  $B^2$  dependence.

Figure 4 shows the shift in a GaAs coupled quantum well structure over a wider range of magnetic fields. At higher field, around 1.0 T, the shift saturates, and at even higher fields, greater than 2–3 T, the luminescence line shifts to higher energy nearly linearly. The magnitude of the shifts depends on the electric field. As discussed in Ref. 5, the linear blueshift at high magnetic field and high electric field can be understood simply in terms of the Landau shift of the electrons and holes. At high electric field, the electrons and holes are pulled to opposite sides of the wells, decreasing the exciton binding energy. When the Landau level energy is large compared to the exciton binding energy, the electrons and holes act nearly independently, and the luminescence energy is simply the sum of the indirect band gap plus the Landau level energy for an electron and a hole.

These effects are in sharp contrast to the magnetic field shifts of excitons in bulk semiconductors or in unbiased quantum wells. In unbiased systems, the exciton luminescence shifts monotonically upward, proportional to  $B^2$  at low magnetic field.<sup>7,8</sup> This shift in single quantum wells is well understood as arising from the diamagnetic response of the excitons. The difference in this case must come from the spatial separation of the electrons and holes in the coupled quantum wells.

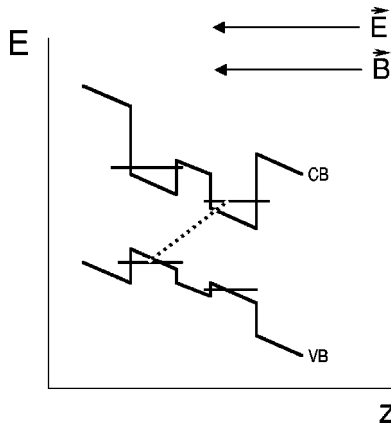


FIG. 1. Model of the bands of the coupled quantum well heterostructure used in this study.

## II. MECHANISM OF THE SHIFT-POSITIVE MAGNETORESISTANCE OF THE TUNNELING BARRIER

At low field, the Landau level energy is negligible compared to the exciton binding energy. Therefore we must look for some effect other than a change of the exciton structure to explain the large energy shift. We have found that this red shift at low field can be understood as arising from a positive magnetoresistance of the structure, which leads to a change in the effective electric field felt by the excitons. This is confirmed by measurement of the current through the structure. Although there are thick barriers in these structures, there is a dc current of the order of  $50 \mu\text{A}$  at high electric field, because the tilting of the bands allows a non-negligible tunneling rate through the barriers, and we use a sample with large surface area, approximately  $4 \text{ mm}^2$ . Figure 5(a) shows a comparison of the measured current and the spectral position of the luminescence in an InGaAs structure as a function

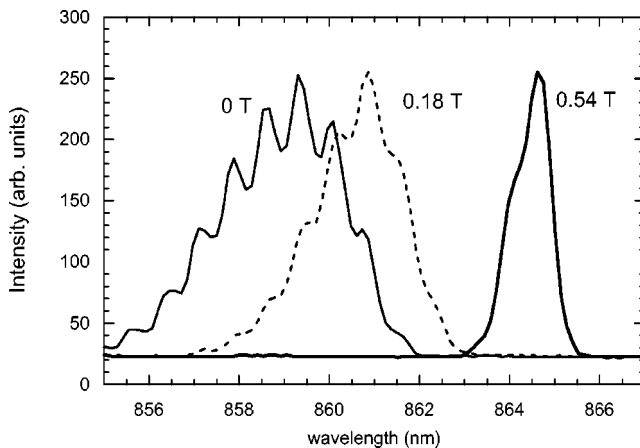


FIG. 2. Indirect exciton luminescence from a coupled quantum well structure with  $\text{In}_{0.1}\text{Ga}_{0.9}\text{As}$  wells and GaAs barrier, for various magnetic fields. The fringes are due to interference from the GaAs substrate, which is transparent at these wavelengths. The sample is placed in liquid helium at  $T=2 \text{ K}$  and illuminated with a low-power ( $\sim 10 \text{ W/cm}^2$ ) laser with wavelength  $847 \text{ nm}$ . The applied electric field is approximately  $69 \text{ kV/cm}$  or  $3.8 \text{ V}$  across the  $5500 \text{ \AA}$  of undoped material.

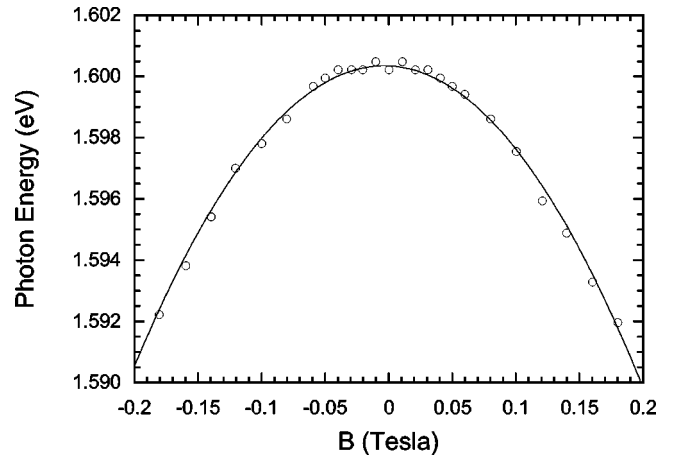


FIG. 3. Photon energy of the luminescence maximum as a function of magnetic field for indirect excitons in a coupled quantum well structure consisting of GaAs quantum wells and  $\text{Al}_{0.3}\text{Ga}_{0.7}\text{As}$  inner barrier. The solid line is a fit to a  $B^2$  dependence. The structure consisted of two coupled GaAs quantum wells of width  $60 \text{ \AA}$ , with an  $\text{Al}_{0.3}\text{Ga}_{0.7}\text{As}$  barrier between the wells of width  $40 \text{ \AA}$ , and outer barriers consisting of  $200 \text{ \AA}$  of  $\text{Al}_{0.3}\text{Ga}_{0.7}\text{As}$ . The sample is placed in liquid helium at  $T=2 \text{ K}$  and illuminated with a low-power ( $\sim 10 \text{ W/cm}^2$ ) laser with wavelength  $632 \text{ nm}$ . The applied electric field is approximately  $30 \text{ kV/cm}$ , or  $2 \text{ V}$  across  $6500 \text{ \AA}$  of undoped material.

of magnetic field. Figure 5(b) shows the change of the overall resistance implied by these data.

The relationship of the spectral position and the current can be understood in terms of a simple two-resistor model, shown in Fig. 6(a). Electric field is applied across the entire sample, while the electric field which affects the luminescence is only the field across the wells. The resistance of this region  $R_w$  is controlled by the tunneling rate through the inner barrier between the wells. The second resistance  $R_0$  includes the contact resistance as well as the resistance of the

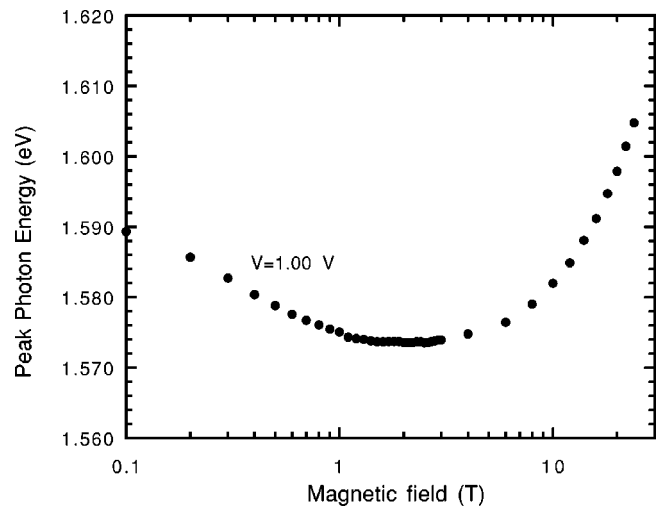


FIG. 4. Photon energy of the luminescence maximum for the same structure and conditions as Fig. 3, but over a wider range of magnetic field, and for applied electric field of  $15 \text{ kV/cm}$ . Note that the horizontal scale is logarithmic.

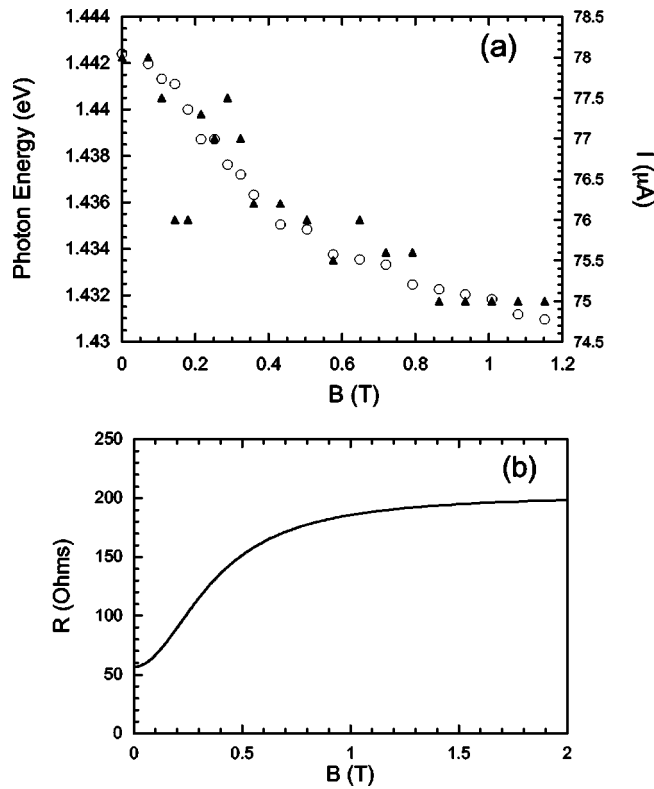


FIG. 5. (a) Open circles: the luminescence line position as a function of magnetic field for the same structure as used for the data of Fig. 2 (left axis.) Triangles: the current measured through the sample under the same conditions (right axis). (b) The resistance implied by these data.

outer barriers, which is much larger than the resistance of the inner barrier. If  $R_w$  increases with magnetic field, then the voltage across  $R_w$  will increase. Because of the quantum-confined Stark effect, an increase of the voltage across the wells will lead to a red shift of the indirect luminescence

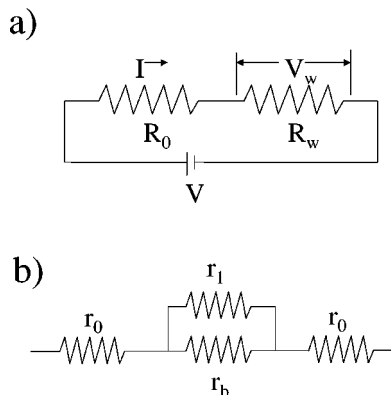


FIG. 6. (a) Two-resistor model of the system of the wells + barriers. When the resistance of the well increases, the total current through the structure drops and the voltage across the wells decreases. (b) The resistor model in which the inner barrier resistance  $R_w$  is replaced by two parallel resistors, representing the different tunneling rates due to disorder, and  $R_0$  is represented by two resistors in series, corresponding to the two outer barriers of the structure.

line. When the voltage across the wells is decreased, the maximum red shift with magnetic field also decreases, because the voltage across  $R_w$  is proportional to the total voltage across the coupled well system, as in a simple voltage divider circuit.

The effect of the line shift with magnetic field is therefore understandable in terms of a positive magnetoresistance of the structure. At first glance, however, it is not obvious why magnetic field should have any effect on the resistance, because there are no magnetic materials in this system, and the applied magnetic field is parallel to the applied electric field.

The mechanism which we propose for the magnetoresistance is qualitatively similar to the mechanism proposed by Lee *et al.*<sup>9</sup> to explain the magnetoresistance of superlattices. The effect occurs at much lower magnetic field in our case, however.

Although the electric field and the magnetic field are parallel, a current exists in the system which flows perpendicular to the magnetic field. Because the resistance in the planes of the wells is much lower than the effective resistance of the barriers, the carriers will undergo diffusion in the wells in the direction perpendicular to the electric and magnetic fields. This diffusion constant in the wells can depend on the magnetic field, since the carriers must move perpendicular to the magnetic field to diffuse.

In all quantum well structures, there is some disorder. This disorder can be seen in the inhomogeneous line broadening of the luminescence. In our samples, the inhomogeneous broadening is between 1 and 3 meV (as seen in Fig. 1, the inhomogeneous linewidth decreases with increasing magnetic field, an effect also seen by Lee and Bajaj.<sup>10</sup>) By comparison, the energy change in the quantized electron states for one monolayer variation of the well width is 6 meV, which means that these quantum wells consist of flat islands which are monolayer perfect over tens to hundreds of microns. Therefore the disorder which leads to the inhomogeneous broadening does not come from well width variations; most likely it arises from random fluctuations in the alloy concentration. In the GaAs quantum wells, the barriers consist of  $\text{Al}_x\text{Ga}_{1-x}\text{As}$  alloy, while in the  $\text{In}_x\text{Ga}_{1-x}\text{As}$  wells, the wells themselves have the alloy fluctuations and the adjacent barriers are pure GaAs.

The fluctuation of the barrier height, especially of the thin, 40 Å barrier between the two wells, leads to spatial variation of the tunneling rate through the barriers. Therefore if the carriers have a high diffusion constant, they can diffuse into regions with lower tunneling time. This will then lower the effective resistance of the barrier to tunneling current.

When magnetic field is applied, the electron and hole orbits become constrained. Even if the radius of the free-carrier Landau orbits is large compared to the excitonic Bohr radius, the effect of the magnetic field will be to deter the carriers from moving to the regions of lowest potential energy; therefore they will feel an average of the well potential instead of local fluctuations. This will slow down the tunneling rate, since the free carriers cannot migrate to regions with high tunneling rate.

### III. THEORETICAL MODEL OF THE MAGNETORESISTANCE

The theory of the magnetoresistance due to this mechanism can be developed in the same way as it has been done for superlattices by Miller and Laikhtman.<sup>11</sup> In this model, the potential at the first contact is  $U$ , the potential in the well separated from this contact by the first barrier is  $\phi_1(\mathbf{r})$ , the potential in the second well is  $\phi_2(\mathbf{r})$ , and the potential of the second contact is  $-U$ . The potentials inside the wells depend on in-plane coordinate  $\mathbf{r}$  because of the nonuniformity of the barriers. Magnetic field is applied in the growth direction ( $z$  direction). If the local conductances of the first, second (intermediate) and third barriers are  $\Sigma_1(\mathbf{r})$ ,  $\Sigma_2(\mathbf{r})$ , and  $\Sigma_3(\mathbf{r})$ , respectively, then the current densities across the barriers are

$$j_{z1}(\mathbf{r}) = \Sigma_1(\mathbf{r})[U - \phi_1(\mathbf{r})], \quad j_{z2}(\mathbf{r}) = \Sigma_2(\mathbf{r})[\phi_1(\mathbf{r}) - \phi_2(\mathbf{r})], \quad j_{z3}(\mathbf{r}) = \Sigma_3(\mathbf{r})[\phi_2(\mathbf{r}) + U]. \quad (3.1)$$

The current conservation law in the first and second wells reads

$$j_{z2} - j_{z1} = \nabla \hat{\sigma} \nabla \phi_1, \quad j_{z3} - j_{z2} = \nabla \hat{\sigma} \nabla \phi_2, \quad (3.2)$$

where  $\nabla$  is the in-plane gradient. The in-plane conductivity tensor of both wells is assumed the same. It is antisymmetric,  $\sigma_{xy} = -\sigma_{yx}$  and the dependence of the diagonal components on the magnetic field is

$$\sigma_{xx} = \sigma_{yy} \equiv \sigma_{\parallel} = \frac{\sigma_0}{1 + (\mu B/c)^2}, \quad (3.3)$$

where  $\sigma_0$  and  $\mu$  are the conductivity and mobility at zero magnetic field. Elimination of  $j_{z1}$  and  $j_{z2}$  from Eqs. (3.1) and (3.2) leads to the equations for the potentials

$$\Sigma_2(\mathbf{r})[\phi_1(\mathbf{r}) - \phi_2(\mathbf{r})] - \Sigma_1(\mathbf{r})[U - \phi_1(\mathbf{r})] = \sigma_{\parallel} \nabla^2 \phi_1, \quad (3.4a)$$

$$\Sigma_3(\mathbf{r})[\phi_2(\mathbf{r}) + U] - \Sigma_2(\mathbf{r})[\phi_1(\mathbf{r}) - \phi_2(\mathbf{r})] = \sigma_{\parallel} \nabla^2 \phi_2. \quad (3.4b)$$

The measured current density can be defined as the current density across the intermediate barrier averaged over the fluctuations

$$\langle j \rangle = \langle j_{z2} \rangle = \langle \Sigma_2(\mathbf{r})[\phi_1(\mathbf{r}) - \phi_2(\mathbf{r})] \rangle. \quad (3.5)$$

If the resistance fluctuations of the barriers can be neglected,  $\Sigma_1 = \Sigma_3 \equiv \Sigma_0 = \text{const}$ ,  $\Sigma_2 = \text{const}$  then Eqs. (3.4) and (3.5) lead to

$$\phi_1 = -\phi_2 = \frac{\Sigma_0}{2\Sigma_2 + \Sigma_0} U \quad (3.6)$$

and

$$j = \frac{2\Sigma_0 \Sigma_2}{2\Sigma_2 + \Sigma_0} U. \quad (3.7)$$

This expression corresponds to total resistance equal to the sum of the barrier resistances  $(1/\Sigma_0) + (1/\Sigma_2) + (1/\Sigma_0)$ .

Due to the large width of the outer barriers compared to the intermediate one,  $\Sigma_2 \gg \Sigma_1, \Sigma_3$ . This inequality allows us to neglect  $\Sigma_1$  and  $\Sigma_3$  compared to  $\Sigma_2$  in Eq. (3.4), and it is reduced to

$$\Sigma_2(\mathbf{r})[\phi_1(\mathbf{r}) - \phi_2(\mathbf{r})] - \Sigma_1(\mathbf{r})U = \sigma_{\parallel} \nabla^2 \phi_1, \quad (3.8a)$$

$$\Sigma_3(\mathbf{r})U - \Sigma_2(\mathbf{r})[\phi_1(\mathbf{r}) - \phi_2(\mathbf{r})] = \sigma_{\parallel} \nabla^2 \phi_2. \quad (3.8b)$$

The difference of these equations gives

$$2\Sigma_2 \phi - \sigma_{\parallel} \nabla^2 \phi = (\Sigma_1 + \Sigma_3)U \quad (3.9)$$

where  $\phi = \phi_1 - \phi_2$ . According to Eq. (3.5)

$$\langle j \rangle = \langle \Sigma_2 \phi \rangle, \quad (3.10)$$

so Eq. (3.9) is enough to find the average current. According to this equation the current is linear in fluctuations of  $\Sigma_1$  and  $\Sigma_3$ , so these fluctuations are averaged out and Eq. (3.9) is reduced to

$$2\Sigma_2 \phi - \sigma_{\parallel} \nabla^2 \phi = 2\Sigma_0 U. \quad (3.11)$$

The average current  $\langle j \rangle$  can be easily calculated when fluctuations of  $\Sigma_2$  are small. In the experiment, however, the resistance of the structure changes by a factor of 3 or more, so that conductance fluctuations are significant. In this case the solution of Eq. (3.11) presents a serious problem, aggravated by the fact that the statistic properties of the fluctuations are not known. Therefore, instead of analytical investigation of Eq. (3.11), we make use of a simple model. We replace the whole structure with the circuit shown in Fig. 6(b), which is slightly extended from the model of Fig. 6(a). Here  $r_0$  is the resistance of the outer barriers,  $r_b$  is the average resistance of the inner, intermediate barrier, and  $r_1$  is the sum of the minimal resistance of the second barrier  $r_m$  and the in-plane resistance. The in-plane resistance can be approximated as  $l^2/\sigma_{\parallel}$ , where  $l$  is a characteristic length scale of the barrier conductance fluctuations. Then the resistance of the intermediate part of the structure that does not include the resistances of the outer barriers is

$$R = \left[ \frac{1}{r_b} + \left( r_m + \frac{l^2}{\sigma_{\parallel}} \right)^{-1} \right]^{-1}. \quad (3.12)$$

With the help of Eq. (3.3), this can be written as

$$\frac{1}{R} = \frac{1}{r_b} + \frac{1}{r_m + r_{\parallel}} \left[ 1 + \frac{r_{\parallel}}{r_m + r_{\parallel}} (\mu B/c)^2 \right]^{-1}, \quad (3.13)$$

where  $r_{\parallel} = l^2/\sigma_0$ .

At low magnetic field,  $[r_{\parallel}/(r_m + r_{\parallel})](\mu B/c)^2 \ll 1$ , Eq. (3.13) gives

$$\frac{1}{R} = \frac{1}{r_b} + \frac{1}{r_m + r_{\parallel}} - \frac{r_{\parallel}}{(r_m + r_{\parallel})^2} (\mu B/c)^2, \quad (3.14)$$

and the minimal resistance, which is reached at zero magnetic field, is  $R_{\min} = r_b(r_m + r_{\parallel})/(r_b + r_m + r_{\parallel})$ . At high magnetic field,  $[r_{\parallel}/(r_m + r_{\parallel})](\mu B/c)^2 \gg 1$ , and

$$R = \frac{r_b r_{\parallel}}{r_{\parallel} + r_b (c/\mu B)^2}, \quad (3.15)$$

and the maximum resistance is therefore  $R_{\max} = r_b$ .

Equation (3.13) has the apparently anomalous implication that if  $r_m = r_b$ , i.e., if there are no fluctuations in the barrier resistance, there is still a magnetoresistance effect. The model clearly breaks down in this limit, but we can think of this limit in the following way: the value of  $(r_b - r_m)$  gives a characteristic distance over which carriers must travel to see a substantial reduction in the barrier resistance; as  $(r_b - r_m)$  decreases, the characteristic distance increases. For Gaussian fluctuations, there will always be a large fluctuation if the size of the system is big enough. As  $r_m$  approaches  $r_b$ , the average distance that the carriers must travel in the lateral direction to see a reduction in the barrier resistance approaches infinity. Therefore one can say that, in principle, there will still be a magnetoresistance effect even in the limit  $r_m$  approaching  $r_b$ , except that this will occur only in the case of an infinite sheet of current with an infinite amount of time to diffuse. This implies that the theoretical model will break down when the distance to a large fluctuation implied by Gaussian statistics is larger than the size of the sample.

Figure 7 shows fits of this magnetoresistance theory to two different structures. To fit the data, we use the relation  $E = E_0 - IR$ , where  $E$  is the indirect exciton luminescence energy from the well,  $E_0$  is the unshifted energy,  $I$  is the current (assumed constant, since, as shown in Fig. 7, the fractional change of the total current is small) and  $R$  is the resistance. Using Eq. (3.13), we have

$$IR = a \frac{1 + bB^2}{1 + cB^2}, \quad (3.16)$$

where  $a$ ,  $b$ , and  $c$  are fit parameters.

The fit of Fig. 7(a) implies  $E_0 = 1.615$  eV, and  $a = 0.0235 \pm 0.00024$ ,  $b = 17.8 \pm 0.97$ , and  $c = 10.0 \pm 0.49$ . The fit of Fig. 7(b) implies  $E_0 = 1.447$  eV, and  $a = 0.0046 \pm 0.00017$ ,  $b = 26.3 \pm 2.5$ , and  $c = 7.3 \pm 0.55$ . These fits imply

$$\frac{r_b}{r_m + r_{\parallel}} = 0.78 \pm 0.18$$

for the GaAs quantum well structure and

$$\frac{r_b}{r_m + r_{\parallel}} = 2.6 \pm 0.61$$

for the InGaAs quantum well structure. In the case of the InGaAs quantum wells, the lattice mismatch of the GaAs and InGaAs alloy leads to dislocations, which increase the potential fluctuations.

#### IV. CONCLUSIONS

We have seen that the large red shift of the indirect exciton luminescence with weak magnetic field arises because of a magnetoresistance effect of the tunneling barrier in these coupled quantum well structures. The effect is surprisingly

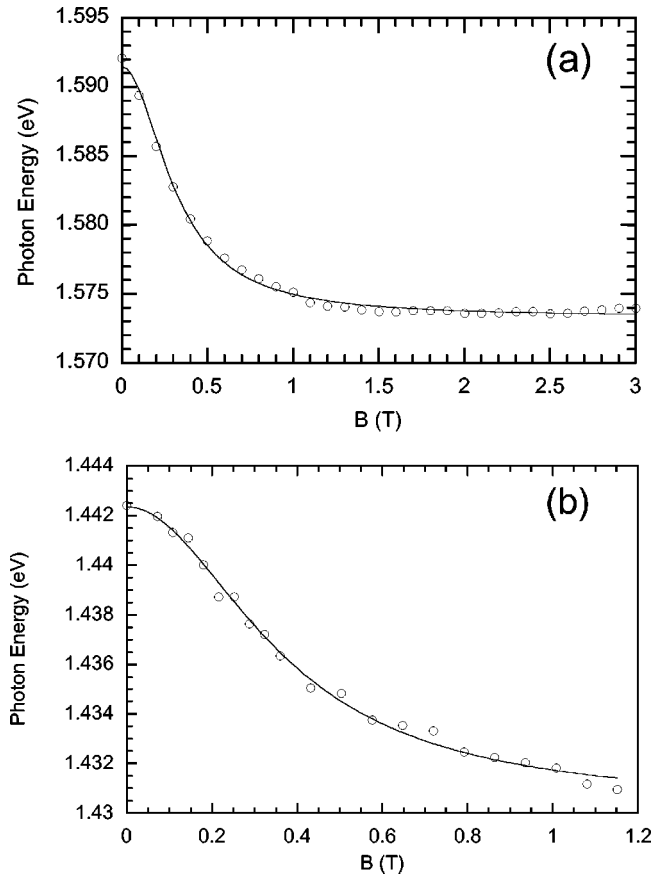


FIG. 7. (a) The photon energy of the luminescence peak vs magnetic field for indirect excitons in the same structure as in Fig. 3, for an electric field of approximately 15 kV/cm. The solid line is a fit to the magnetoresistance theory discussed in the text. (b) A fit of the same theory to the data from the same structure used in Figs. 2 and 5. The sample is illuminated with a low-power laser at 850 nm.

large, corresponding to a factor of 3 increase of the effective resistance, so that it may be termed a “giant” magnetoresistance effect. This effect is observable because the energy position of the indirect excitons is a sensitive measure of the local electric field, and this electric field in turn depends linearly on the current through the sample, because the wells which contain the excitons are in series with a much larger resistance.

*Applications.* Although this effect does not have greater sensitivity to magnetic field than other methods, the fact that the magnetic field gives a direct optical signature leads to the possibility of novel applications. Because the method involves a thin film which can be deposited on many types of surface, large surface areas could be optically interrogated without moving the medium. For example, instead of moving a magnetic recording medium past a single-point detector, the medium could be held fixed, and a focused laser beam could be scanned across its surface at very high speeds using electro-optical scanning methods. Since the luminescence signal arises only where the laser excites the surface, the spectral signature of the light emission at each point in time as the laser scans the surface would provide magnetic



field readout without need for pinpoint imaging of the luminescence. Alternatively, this type of optical detection could allow parallel readout of many channels through normal optical imaging methods. It would be possible to illuminate an entire surface and record an image of the light emission from the epitaxial layer, which would provide a direct, real-time map of a magnetic field distribution.

These results have been obtained at low temperature  $T=2$  K, but because the effect does not depend crucially on low-temperature or excitonic effects, this effect can in principle be extended to room temperature. At very high temperature, the diffusion constant of the carriers may be so low due to phonon scattering that the magnetic field effect may

make little difference. Further studies are needed to determine if this effect can be observed at room temperature.

#### ACKNOWLEDGMENTS

. This work has been supported by the National Science Foundation under Grant No. DMR-0102457, by the Department of Energy under Grant No. DE-FG02-99ER45780, and by the Israel Science Foundation under Grant No. 174/98. Some measurements were performed at the National High Magnetic Field Laboratory (NHMFL), which is supported by NSF Cooperative Agreement No. DMR-9527035. We thank Xing Wei and Bruce Brandt for their help. We also thank Rene Hurka for early contributions to these experiments.

---

\*Present address: TRUMPF Inc., Farmington Industrial Park, Farmington, CT 06032.

†Email address: snoke@pitt.edu

<sup>1</sup>S.R. Andrews, C.M. Murray, R.A. Davies, and T.M. Kerr, *Phys. Rev. B* **37**, 8198 (1988).

<sup>2</sup>A.M. Fox, D.A.B. Miller, G. Livescu, J.E. Cunningham, and W.Y. Yan, *Phys. Rev. B* **44**, 6231 (1991).

<sup>3</sup>Y. Kato, Y. Takahashi, S. Fukatsu, Y. Shiraki, and R. Ito, *J. Appl. Phys.* **75**, 7476 (1994).

<sup>4</sup>V. Negoita, D.W. Snoke, and K. Eberl, *Phys. Rev. B* **60**, 2661 (1999).

<sup>5</sup>V. Negoita, D.W. Snoke, and K. Eberl, *Solid State Commun.* **113**, 437 (2000).

<sup>6</sup>V.V. Krivolapchuk, D.A. Mazurenko, E.S. Moskalenko, N.K. Poletaev, A.L. Zhmpdikov, T.S. Cheng, and C.T. Foxton, *Phys. Solid State* **5**, 737 (1998).

<sup>7</sup>K. Oettinger, A.L. Efros, B.K. Meyer, C. Woelk, and H. Brugger, *Phys. Rev. B* **52**, R5531 (1995).

<sup>8</sup>Q.X. Zhao, B. Monemar, P.O. Holtz, M. Willander, B.O. Fimland, and K. Johannensen, *Phys. Rev. B* **50**, 4476 (1994).

<sup>9</sup>M. Lee, N.S. Wingreen, S.A. Solin, and P.A. Wolff, *Solid State Commun.* **89**, 687 (1994).

<sup>10</sup>S.M. Lee and K.K. Bajaj, *J. Appl. Phys.* **73**, 1788, (1993).

<sup>11</sup>D.L. Miller and B. Laikhtman, *Phys. Rev. B* **54**, 10 669 (1996).